QUARTERLY OF APPLIED MATHEMATICS
VOLUME LXIII, NUMBER 1
MARCH 2005, PAGES 34–55
S 0033-569X(04)00938-6
Article electronically published on December 17, 2004

STABILITY OF NEGATIVE STIFFNESS VISCOELASTIC SYSTEMS

By

YUN-CHE WANG (*Department of Engineering Physics, Engineering Mechanics Program, University of Wisconsin-Madison, 147 Engineering Research Building, 1500 Engineering Drive, Madison, WI 53706-1687*)

and

RODERIC LAKES (*Department of Engineering Physics, Engineering Mechanics Program, Biomedical Engineering Department; Materials Science Program and Rheology Research Center, University of Wisconsin-Madison, 147 Engineering Research Building, 1500 Engineering Drive, Madison, WI 53706-1687*)

Abstract. We analytically investigate the stability of a discrete viscoelastic system with negative stiffness elements both in the time and frequency domains. Parametric analysis was performed by tuning both the amount of negative stiffness in a standard linear solid and driving frequency. Stability conditions were derived from the analytical solutions of the differential governing equations and the Lyapunov stability theorem. High frequency response of the system is studied. Stability of singularities in the dissipation $\tan\delta$ is discussed. It was found that stable singular $\tan\delta$ is achievable. The system with extreme high stiffness analyzed here was metastable. We established an explicit link for the divergent rates of the metastable system between the solutions of differential governing equations in the time domain and the Lyapunov theorem.

1. Nomenclature.

M, m_1, m_2: mass.
K, k_1, k_2: stiffness for positive stiffness elements.
c, c_1, c_2: damping coefficient.
α, α_1, α_2: ratio between the two spring elements in a standard linear solid. $\alpha = \alpha_1$ when $\alpha_2 = 0$.
γ_1, γ_2: ratio of damping coefficient of a standard linear solid to that of a damper parallel-connected to the standard linear solid, i.e., $\gamma = \eta/c$.
δ: phase angle. Define $\tan\delta = \Im(k^*)/\Re(k^*)$, where k* denotes the dynamic complex spring constant.
κ_1, κ_2: ratio of stiffness of the series spring in a standard linear solid to that of a spring parallel-connected to the standard linear solid, i.e., $\kappa = y/k$.

Received December 15, 2003.
2000 *Mathematics Subject Classification.* Primary 74B10; Secondary 74C10, 74D05.
E-mail address: lakes@engr.wisc.edu

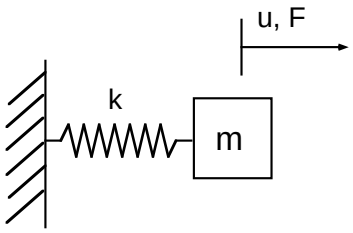

FIG. 1. Spring-mass system, one degree of freedom (dof).

y, y_1, y_2, z, z_1, z_2: stiffness for standard linear solid elements, to be tuned. $y_1 = \kappa_1 k_1$, $y_2 = \kappa_2 k_2$, $y = y_1$, $z = z_1$.
η, η_1, η_2: damping coefficient for standard linear solids. $\eta_1 = \gamma_1 c_1$, $\eta_2 = \gamma_2 c_2$, $\eta = \eta_1$.
u, u_1, u_2: displacement coordinate of a node.
$\dot{u} : \frac{du}{dt}$.
F, F_1, F_2: applied force at a node.
ω, Ω: frequency.
H: Hamiltonian.
D: differential operator, $\frac{d}{dt}$.
h: superscript, homogeneous solutions of a differential equation.
p: superscript, particular solutions of a differential equation.
subscripts: labels of components in a model.

2. Introduction. A bulk solid object of negative stiffness materials is not stable. However, it might be possible to create a stable configuration for composites with a negative stiffness component embedded. Extreme material properties and stability-related issues have been reported in [3]–[6] and [11]–[14]. Here, we first review the stability of a simple discrete mechanical model, a spring-mass system, to mathematically demonstrate its internal stability [9] and the stability under external excitations. Then we investigate the stability of systems with negative stiffness components. This single degree of freedom (dof) system is shown in Figure 1.

By Newton's second law, the equation of motion is

$$m\ddot{u} + ku = F, \tag{1}$$

where m is the mass, k the stiffness, $u = u(t)$ the displacement, and $F = F(t)$ the external driving force. A superdot indicates the derivative with respect to time. The solution of the equation of motion in the time domain is as follows. Assume $F = P + A\cos\Omega t$ and P and A are constants.

$$u = u^h + u^p, \tag{2}$$

where the homogeneous solution $u^h = C_1 e^{\lambda_1 t} + C_2 e^{\lambda_2 t}$, where $\lambda_{1,2} = \pm i\omega$ and $\omega^2 = k/m$, and C_1 and C_2 are constants to be determined by initial conditions. As for the particular

solutions, u^p, one can express them as follows.

$$u^p = \frac{P}{k} + \frac{A\cos\Omega t}{-m\Omega^2 + k}, \quad \text{when} \quad \Omega \neq \omega. \tag{3}$$

$$u^p = \frac{P}{k} + \frac{t}{2\Omega} A\sin\Omega t, \quad \text{when} \quad \Omega = \omega. \tag{4}$$

It is clear to see that instability occurs only when $\Omega = \omega$, due to time-growing behavior in its particular solution. Therefore, from this time domain analysis, the stability criterion is that the system is stable when $\Omega \neq \omega$. This stability criterion can also be obtained through analysis in the frequency domain. Applying a Fourier transform on Eq. (1), one converts the governing equation into an algebraic equation, as follows.

$$\frac{\widetilde{u}}{\widetilde{F}} = \frac{1}{-m\omega^2 + k}. \tag{5}$$

The instability of the system occurs only when $\omega^2 = k/m$, which is consistent with previous results from Eq. (4). Furthermore, the results indicate that the system is internally stable when $F = 0$ and $k/m > 0$. Moreover, the system is also stable when $k < 0$ and $m < 0$. For $k/m < 0$, there are no oscillatory solutions for the system, only real exponential ones. Hence, it is internally unstable.

The internal stability is the stability of a system under no external forcing. However, in some cases, it is important to investigate a dynamical system with time variables explicitly (i.e., non-autonomous systems), such as flutter analysis. A general method for attacking this problem is to consider the time variable as an ordinary spatial variable [10]. However, by doing so, the Lyapunov indirect method will not be suitable for stability analysis since it is local. The Lyapunov direct method can be applied, but stability must be checked at all times in the time domain [8].

Alternatively, one can rigorously derive the stability criteria of a mechanical system by using the so-called extended energy method [7]. Using the system depicted in Eq. (1) as an example, we first rewrite the equation of motion for the system as follows.

$$\ddot{q} + \omega^2 q = \frac{A}{m}\cos\Omega t \tag{6}$$

where $q = q(t)$ is the generalized coordinate, ω^2 the ratio of k to m, and Ω the driving frequency. $q(t)$ is different from $u(t)$ in that the latter contains the contribution from the dead load P. The total energy of the system can be calculated as follows.

$$E = \int_0^t (\ddot{q} + \omega^2 q - \frac{A}{m}\cos\Omega t)\dot{q}dt = \frac{1}{2}\dot{q}^2 + \frac{1}{2}\omega^2 q^2 - \int_0^t (\frac{A}{m}\cos\Omega t)\dot{q}dt. \tag{7}$$

It is clear to see that the energy is not a first integral of the system. From Eq. (7), it is understood that the Hamiltonian and non-conservative force can be written as follows.

$$H = \frac{1}{2}p^2 + \frac{1}{2}\omega^2 q^2, \quad \textit{and} \tag{8}$$

$$N = \frac{A}{m}\cos\Omega t. \tag{9}$$

Here $p = \dot{q}$. Define $\phi = \phi(q, \lambda, \Omega) = dE$, and, for $E = E(q, p, \Omega)$, the explicit representations of ϕ and $d\phi$ are as follows.

$$\phi = \frac{\partial H}{\partial q} - N + G = 0, \quad G = \frac{\partial H}{\partial p}\frac{dp}{dq} \tag{10}$$

$$d\phi = \frac{\partial \phi}{\partial q}dq + \frac{\partial \phi}{\partial \lambda}d\lambda + \frac{\partial \phi}{\partial \Omega}d\Omega = 0 \tag{11}$$

or

$$(\frac{\partial^2 H}{\partial q^2} - \frac{\partial N}{\partial q} + \frac{\partial G}{\partial q})dq + (\frac{\partial G}{\partial \lambda} - \frac{\partial N}{\partial \lambda})d\lambda + (\frac{\partial^2 H}{\partial \Omega \partial q} - \frac{\partial N}{\partial \Omega})d\Omega = 0. \tag{12}$$

Here λ is the characteristic frequency of the system. In the present case, λ is chosen to be Ω, and Ω is the control parameter in the stability analysis, which means the results of the stability analysis will indicate a specific value or region for Ω to make the system unstable. In order to calculate ϕ in terms of λ explicitly, we assume the solution for q as follows.

$$q = B\cos(\lambda t + \Phi) = B\cos(\Omega t + \Phi). \tag{13}$$

Here B and Φ are to be determined. Consequently, p can be found as follows.

$$p = \dot{q} = -B\Omega\sin(\Omega t + \Phi) = -\Omega\sqrt{B^2 - q^2}. \tag{14}$$

Thus, the G in Eq. (12) can be calculated as follows.

$$G = p\frac{dp}{dq} = (-\Omega\sqrt{B^2 - q^2})(-\Omega\frac{1}{2}\frac{1}{\sqrt{B^2 - q^2}}(-2q)) = \Omega^2 q. \tag{15}$$

When the instability occurs, $dq/dq = \infty$. The instability occurs when the following equation is satisfied.

$$\frac{\partial^2 H}{\partial q^2} - \frac{\partial N}{\partial q} + \frac{\partial G}{\partial q} = 0, \quad or \quad \omega^2 - \Omega^2 = 0. \tag{16}$$

Clearly, Eq. (16) suggests the system is unstable only when the driving frequency is equal to the natural frequency of the system, as expected.

The above results can be generalized to the problem with many degrees of freedom. With external excitations, a system becomes unstable when the driving frequency coincides with one of the natural frequencies of the system. However, the system can be stabilized in the sense that no unbounded responses occur when damping elements are included. Without driving force, the system is internally stable when both mass and stiffness are positive or negative. Following the similar spirit in Eqs. (2)–(5), we explore the stability of the 2-dof viscoelastic models, shown in Figure 2, with negative stiffness elements under external excitations, and cross-link our results with the Lyapunov indirect theorem.

3. Equations of motion. The mechanical system considered here is shown as Figure 2(a), in which the left module is called element 1, and the right one is called element 2. Figure 2(b) is a simplified version of Figure 2(a), intended to be used in later parametric study. The subscripts indicate to which module a component belongs. The mass points m_1 and m_2 are called node 1 and node 2, respectively. Following Newton's second law, the equations of motion of the mechanical system can be expressed as follows.

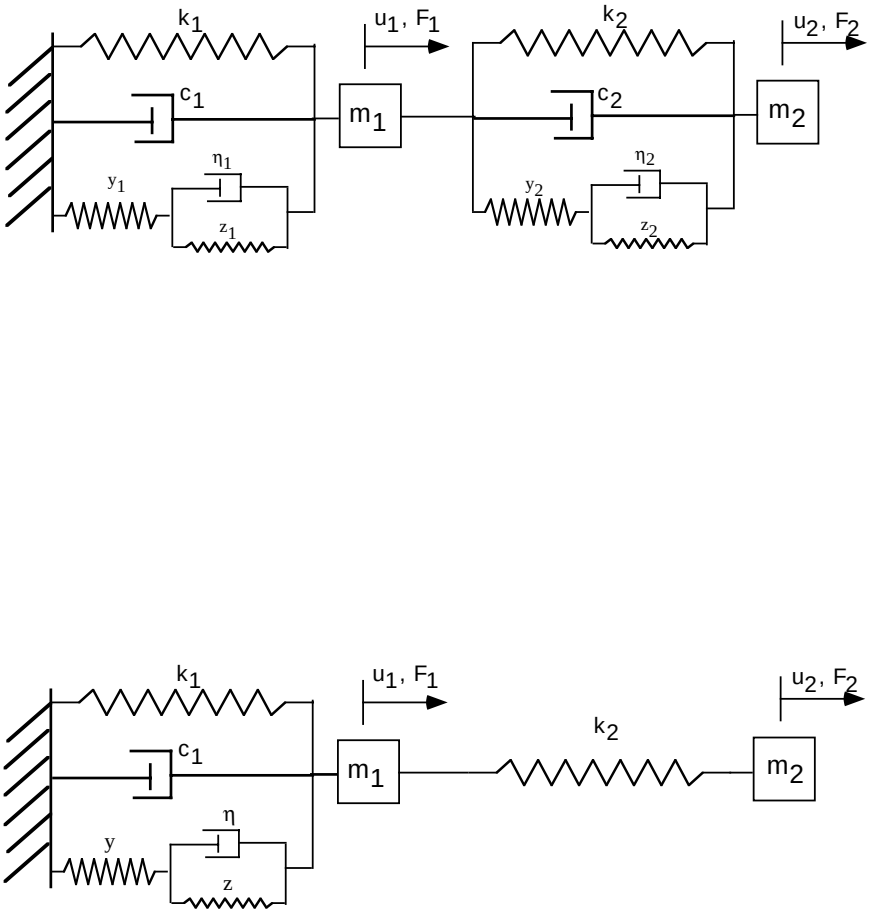

FIG. 2. (a) The 2-dof viscoelastic model. (b) The simplified version of (a), used in parametric study.

$$\begin{bmatrix} m_1 & 0 \\ 0 & m_2 \end{bmatrix} \begin{pmatrix} \ddot{u}_1 \\ \ddot{u}_2 \end{pmatrix} + \begin{bmatrix} c_1+c_2 & -c_2 \\ -c_2 & c_2 \end{bmatrix} \begin{pmatrix} \dot{u}_1 \\ \dot{u}_2 \end{pmatrix} + \begin{bmatrix} k_1+k_2 & -k_2 \\ -k_2 & k_2 \end{bmatrix} \begin{pmatrix} u_1 \\ u_2 \end{pmatrix} + \begin{pmatrix} f_1-f_2 \\ f_2 \end{pmatrix} = \begin{pmatrix} F_1 \\ F_2 \end{pmatrix} \quad (17)$$

where

$$f_1 + \frac{\gamma_1 c_1}{y_1+\alpha_1 y_1}\dot{f}_1 = \frac{\alpha_1 y_1^2}{y_1+\alpha_1 y_1}u_1 + \frac{y_1\gamma_1 c_1}{y_1+\alpha_1 y_1}\dot{u}_1, \quad (18)$$

$$f_2 + \frac{\gamma_2 c_2}{y_2+\alpha_2 y_2}\dot{f}_2 = \frac{\alpha_2 y_2^2}{y_2+\alpha_2 y_2}(u_2-u_1) + \frac{y_2\gamma_2 c_2}{y_2+\alpha_2 y_2}(\dot{u}_2-\dot{u}_1), \quad (19)$$

are the constitutive equations for the internal force and deformation in the standard linear solids (i.e., the $y_1-\eta_1-z_1$ or $y_2-\eta_2-z_2$ module). The symbols f_1 and f_2 denote the internal force in the standard linear solid elements. Also, we define $y_i=\kappa_i k_i$, $\eta_i=\gamma_i c_i$ and $z_i=\alpha_2 y_i$, where $i=1,2$, to facilitate our later parametric study.

3.1. *Solutions in the frequency domain.* Investigating the solutions of the equations is helpful in understanding the response of the systems at different frequency. After Fourier transform, the governing equations of the system, Eqs. (17)–(19), can be converted into the following algebraic equations.

$$\mathbf{T}\begin{pmatrix} \widetilde{u}_1 \\ \widetilde{u}_2 \end{pmatrix} = \begin{pmatrix} \widetilde{F}_1 \\ \widetilde{F}_2 \end{pmatrix}, \quad (20)$$

where

$$\mathbf{T} = \begin{bmatrix} -\omega^2 m_1 + k_1 + k_2 + i\omega(c_1+c_2) + d_1 + d_2 & -(k_2+i\omega c_2) - d_2 \\ -(k_2+i\omega c_2) - d_2 & -\omega^2 m_2 + k_2 + i\omega c_2 + d_2 \end{bmatrix}, \quad (21)$$

$$d_1 = \frac{\alpha_1 y_1^2 + i\omega y_1\gamma_1 c_1}{y_1+\alpha_1 y_1 + i\omega\gamma_1 c_1}, \quad (22)$$

$$d_2 = \frac{\alpha_2 y_2^2 + i\omega y_2\gamma_2 c_2}{y_2+\alpha_2 y_2 + i\omega\gamma_2 c_2}. \quad (23)$$

It is noted that the determinant of the coefficient matrix, Eq. (21), dominates the boundedness of the displacement responses in frequency domain. In other words, if the coefficient matrix becomes singular, the system will be unstable in the sense that finite input produces unbounded output. However, it is not required for $\mathbf{T}$ to be positive definite for stability. We remark that for gyroscopic systems, $\mathbf{T}$ is not symmetric, as discussed in [1], [2], [7] and references therein. One usually encounters gyroscopic systems when follower forces are considered. Our system is not gyroscopic. The effective complex compliance (j_{eff}) and effective stiffness (k_{eff}) can be calculated at a specified frequency as follows.

$$j_{eff} = j'_{eff} + j''_{eff} = \frac{\widetilde{u}_2}{\widetilde{F}_2}, \quad \textit{and} \quad (24)$$

$$k_{eff} = k'_{eff} + k''_{eff} = \frac{\widetilde{F}_2}{\widetilde{u}_2}. \quad (25)$$

The effective $\tan\delta$ is defined as follows.

$$\tan\delta = \frac{k''_{eff}}{k'_{eff}}, \quad or \quad \tan\delta = -\frac{j''_{eff}}{j'_{eff}}. \tag{26}$$

For the special case $m_1 = m_2 = 0$, $c_1 = c_2 = 0$, $y_2 = 0, k_1 = 10$, and $k_2 = 5$ kN/m, the overall $\tan\delta$ can be obtained from $\tan\delta = h/g$, where

$$h(y, z, \eta, \omega) = 5\omega\eta y^2 A^2, \tag{27}$$

$$g(y, z, \eta, \omega) = (\omega^2\eta^2 + z^2)(\omega^2\eta^2 + (y+z)^2) + 25y(\omega^2\eta^2 + z(y+z))A^2 + 150y^2A^4, \tag{28}$$

$$A = \left|1 + \frac{z}{y} + i\frac{\omega\eta}{y}\right|. \tag{29}$$

Here $z = \alpha y$. Choosing zero masses is done to reduce some mathematical complexities, and at the same time, simulates a composite material in the continuum sense. This is the special case studied in [13]. Later, we will discuss some interesting singular behavior of the overall $\tan\delta$ for this special case.

3.2. *Solutions in the time domain.* The general solution of Eq. (17) in the time domain is quite complicated. For the purpose of demonstrating extreme properties of the mechanical system due to a negative stiffness element, we assume $c_2 = 0$, $\kappa_2 = 0$, and $\gamma_2 = 0$, as shown in Figure 2 (b). One should be aware that artificially setting material properties to be zero causes certain degrees of degeneracy in solutions. We will point out the effects of degeneracy along with our derivation. The governing equation can be expressed as follows.

$$\begin{bmatrix} m_1 & 0 \\ 0 & m_2 \end{bmatrix}\begin{pmatrix} \ddot{u}_1 \\ \ddot{u}_2 \end{pmatrix} + \begin{bmatrix} c_1 & 0 \\ 0 & 0 \end{bmatrix}\begin{pmatrix} \dot{u}_1 \\ \dot{u}_2 \end{pmatrix} + \begin{bmatrix} k_1+k_2 & -k_2 \\ -k_2 & k_2 \end{bmatrix}\begin{pmatrix} u_1 \\ u_2 \end{pmatrix} + \begin{pmatrix} f_1 \\ 0 \end{pmatrix} = \begin{pmatrix} F_1 \\ F_2 \end{pmatrix}. \tag{30}$$

To decouple the above equation, one multiplies the inverse of the stiffness matrix (non-singular stiffness matrix is assumed) on the both sides of the equation, and then obtains the following.

$$\begin{bmatrix} \frac{m_1}{k_1} & \frac{m_2}{k_1} \\ \frac{m_2}{k_1} & \frac{k_1+k_2}{k_1k_2}m_2 \end{bmatrix}\begin{pmatrix} \ddot{u}_1 \\ \ddot{u}_2 \end{pmatrix} + \begin{bmatrix} \frac{c_1}{k_1} & 0 \\ \frac{c_1}{k_1} & 0 \end{bmatrix}\begin{pmatrix} \dot{u}_1 \\ \dot{u}_2 \end{pmatrix} + \begin{bmatrix} 1 & 0 \\ 0 & 1 \end{bmatrix}\begin{pmatrix} u_1 \\ u_2 \end{pmatrix} + \begin{pmatrix} \frac{f_1}{k_1} \\ \frac{f_1}{k_1} \end{pmatrix} = \begin{pmatrix} \frac{F_1}{k_1} + \frac{F_2}{k_1} \\ \frac{F_1}{k_1} + \frac{k_1+k_2}{k_1k_2}F_2 \end{pmatrix}. \tag{31}$$

It can be seen that the above equation is not fully decoupled yet. However, if one makes a further assumption that $m_1 = m_2 = 0$, the equations can be decoupled as follows.

$$\dot{u}_1 + \frac{k_1}{c_1}u_1 + \frac{f_1}{c_1} = \frac{1}{c_1}(F_1 + F_2), \tag{32}$$

$$\dot{u}_2 + \frac{k_1}{c_1}u_2 + \frac{f_1}{c_1} = \frac{F_1}{c_1} + \frac{k_1+k_2}{c_1k_2}F_2, \tag{33}$$

where

$$f_1 = e^{\frac{-y_1(1+\alpha_1)t}{\eta_1}} \left[\int_0^t (\frac{\alpha_1 y_1^2}{\gamma_1 c_1} u_1 + y_1 \dot{u}_1) e^{\frac{y_1(1+\alpha_1)t}{\eta_1}} dt + f_1(0) \right]. \tag{34}$$

The zero mass assumption is implemented in later numerical study by assigning $m_1 = m_2 = 10^{-8}$. Also, the assumption is legitimate in our study since the analysis is intended to model composites in the continuum sense. Note again, by doing so, m-degeneracy is unavoidable. Appendix A shows the effects of the m-degeneracy through a 1-dof example. Eq. (34) is the solution of Eq. (18). $f_1(0)$ is the initial condition, equal to $y_2 u_1(0)$. Observing Eq. (33), it can be found that the solution of u_2 is completely determined by that of u_1, as in Eq. (35). From now on, we assume $F_1 = 0$ throughout the rest of the analysis. The physical rationale is to simulate the mechanical behavior of two phase composites, in which the interface between the two phases has no external force applied independent of the solid phases.

$$u_2 = e^{\frac{-k_1 t}{c_1}} \left[\int_0^t (\frac{k_1 + k_2}{c_1 k_2} F_2 - \frac{f_1}{c_1}) e^{\frac{k_1 t}{c_1}} dt + u_2(0) \right]. \tag{35}$$

As for the solution of u_1, one introduces Eq. (34) into Eq. (32), and differentiates both sides of the equation with respect to time to eliminate the integral from f_1.

$$c_1 \ddot{u}_1 + (k_1 + y_1 + \frac{y_1(1+\alpha_1)}{\gamma_1}) \dot{u}_1 + (\frac{k_1 y_1 (1+\alpha_1)}{\gamma_1 c_1} + \frac{\alpha_1 y_1^2}{\gamma_1 c_1}) u_1 = \frac{y_1(1+\alpha_1)}{\gamma_1 c_1} F_2 + \dot{F}_2. \tag{36}$$

Eq. (36) is a second-order constant coefficient ordinary differential equation with non-homogeneous (or forcing) terms. Let $F_2 = P_2 + A_2 \cos \Omega_2 t$; one can find the general solution as follows. P_2 and A_2 are pre-chosen constants.

$$u_1 = u_1^h + u_1^p, \tag{37}$$

$$u_1^h = C_1 e^{\lambda_1 t} + C_2 e^{\lambda_2 t}, \tag{38}$$

where

$$\lambda_{1,2} = \frac{-(k_1 + y_1 + \frac{y_1(1+\alpha_1)}{\gamma_1}) \pm \sqrt{(k_1 + y_1 + \frac{y_1(1+\alpha_1)}{\gamma_1})^2 - 4(\frac{k_1 y_1 (1+\alpha_1)}{\gamma_1} + \frac{\alpha_1 y_1^2}{\gamma_1})}}{2c_1}, \tag{39}$$

$$u_1^p = \frac{y_1(1+\alpha_1)}{\gamma_1 c_1} \left[\frac{1}{\lambda_1 \lambda_2} P_2 + \frac{A_2}{\Omega_2^2 + \lambda_2^2} (\frac{\lambda_1 \lambda_2 - \Omega_2^2}{\Omega_2^2 + \lambda_1^2} \cos \Omega_2 t + \frac{(\lambda_1 \lambda_2) \Omega_2}{\Omega_2^2 + \lambda_1^2} \sin \Omega_2 t) \right] - \frac{1}{(D - \lambda_1)(D - \lambda_2)} \dot{F}_2. \tag{40}$$

Here, D is the differential operator, defined as d/dt. In the solution, C_1 and C_2 are constants to be determined by initial conditions, and the particular solution can be carried out more explicitly. However, it is enough for stability discussion.

Observe that if $c_1 = 0$, the solution of Eq. (36) is

$$u_1 = e^{\frac{-k_1 y_1 (1+\alpha_1) - \alpha_1 y_1^2}{\eta_1 (k_1 + y_1)}} \left[\int_0^t \frac{\dot{F}_2}{k_1 + y_1} e^{\frac{k_1 y_1 (1+\alpha_1) + \alpha_1 y_1^2}{\eta_1 (k_1 + y_1)}} dt + u_1(0) \right], \quad where \quad k_1 + y_1 \neq 0. \tag{41}$$

Consequently, following Eq. (33),

$$u_2 = \frac{k_1 + k_2}{k_1 k_2} F_2 - \frac{f_1}{k_1}, \tag{42}$$

where f_1 is determined by Eq. (34). It noted that when $k_1 + y_1 = 0$, u_1 becomes unbounded, and so does u_2 consequently. Based on the solutions for the displacements, Eqs. (34) and (41), one can define two time constants, as follows.

$$\tau_1 = \frac{\eta(k_1 + y)}{k_1 y(1+\alpha) + \alpha y^2}, \quad for \quad u_1. \tag{43}$$

$$\tau_2 = \frac{\eta}{y(1+\alpha)}, \quad for \quad u_2. \tag{44}$$

It is noted that Eq. (43) is the relationship between the time constant and the rate of overall divergence for the system, as discussed in [14] by using the Lyapunov indirect method. As for $c1 \neq 0$, the solutions of Eqs. (32) and (33) are more complicated, and can be shown as follows, when $F_1 = 0$.

$$u_1 = C_1 e^{\lambda_1 t} + C_2 e^{\lambda_2 t} + u_1^p, \quad and \tag{45}$$

$$u_2 = e^{\frac{-k_1 t}{c_1}} \left[\int_0^t (\frac{k_1 + k_2}{c_1 k_2} F_2 - \frac{f_1}{c_1}) e^{\frac{k_1 t}{c_1}} dt + u_2(0) \right], \tag{46}$$

where

$$\lambda_{1,2} = \frac{-(k_1 + y_1 + \frac{c_1 y_1 (1+\alpha_1)}{\eta}) \pm \sqrt{(k_1 + y_1 + \frac{c_1 y_1 (1+\alpha_1)}{\eta})^2 - 4c_1 (\frac{k_1 y_1 (1+\alpha_1)}{\eta} + \frac{\alpha_1 y_1^2}{\eta})}}{2c_1}, \tag{47}$$

$$f_1 = e^{\frac{-y_1(1+\alpha_1)}{\eta}} \left[\int_0^t (\frac{\alpha_1 y_1^2}{\gamma_1 c_1} u_1 + y_1 \dot{u}_1) e^{\frac{y_1(1+\alpha_1)}{\eta}} dt + f_1(0) \right]. \tag{48}$$

Similarly, time constants for the solutions can be defined as follows.

$$\tau_0 = -\frac{1}{\lambda_1} \quad and \quad \tau_1 = -\frac{1}{\lambda_2}, \quad for \quad u_1, \tag{49}$$

$$\tau_2 = \frac{\eta_1}{y_1(1+\alpha_1)}, \quad for \quad u_2. \tag{50}$$

If the time constant is positive, the solution, corresponding to the relevant degree of freedom, is exponentially decaying. Negative time constants indicate instability. The applied force (F_2) and particular solution (u_1^p) do not change the boundedness of the solutions if F_2 is a bounded function with respect to time.

4. Stability analysis. It is understood that the Lyapunov indirect method, or Routh-Hurwitz criterion, for stability analysis is based on a first order approximation. In other words, if a system fails the stability test with the Lyapunov indirect method, the response of the system is unbounded under infinitesimal perturbation. However, the rate of divergence may be controllable. For the mechanical system, as shown in Figure 2(b), one needs to find the eigenvalues of the Jacobian matrix of Eq. (51), which is derived from Eqs. (17)–(19) through the state-space technique [8] with $\kappa_2 = 0$ and $\gamma_2 = 0$. Then,

by tuning the parameters y, η, and α, we identify that the regimes containing eigenvalues with positive real part are unstable. α is a dimensionless parameter, defined as $\alpha = z/y$.

$$\begin{pmatrix} \dot{u}_1 \\ \dot{u}_2 \\ \dot{v}_1 \\ \dot{v}_2 \\ \dot{f} \end{pmatrix} = \begin{bmatrix} 0 & 0 & 1 & 0 & 0 \\ 0 & 0 & 0 & 1 & 0 \\ -\frac{k_1+k_2}{m_1} & \frac{k_2}{m_1} & -\frac{c_1+c_2}{m_1} & \frac{c_2}{m_1} & -\frac{1}{m_1} \\ \frac{k_2}{m_2} & -\frac{k_2}{m_2} & \frac{c_2}{m_2} & -\frac{c_2}{m_2} & 0 \\ \frac{\alpha y^2}{\eta} & 0 & y & 0 & -\frac{y(1+\alpha)}{\eta} \end{bmatrix} \begin{pmatrix} u_1 \\ u_2 \\ v_1 \\ v_2 \\ f \end{pmatrix} + \begin{pmatrix} 0 \\ 0 \\ \frac{F_1}{m_1} \\ \frac{F_2}{m_2} \\ 0 \end{pmatrix}. \quad (51)$$

However, since the solutions for the system, shown in Figure 2 (b), have been explicitly derived, as expressed in Eqs. (41) and (42) for $c_1 = 0$, or Eqs. (45) and (46) for $c_1 \neq 0$, one can examine the stability of the system via the boundedness of the solutions as time approaches infinity. Direct investigating the boundedness of the solutions is equivalent to Lyapunov indirect method for stability analysis. The major benefit of investigating the solutions in the time domain is that the stability analysis can be done in a more transparent manner. Later, in our parametric study, we directly solve the eigenvalues of the Jacobian matrix in Eq. (51). It has been identified that the time constant in Eq. (43) is responsible for the only eigenvalue with positive real part in the Jacobian matrix, as discussed in [14]. In the following, we derive stability criteria on the physical quantities of our model from the solutions in the time domain. First, for $c_1 \neq 0$, from Eq. (46), the conditions for u_2 to be bounded are as follows.
(a) $k_1/c_1 > 0$, so that there will be no exponentially growing behavior due to $u_2(0)$.
(b) $f_1(t)$ and $F_2(t)$ need to be non-exponentially growing functions, such as constant, trigonometric functions, or exponentially decaying functions.

In contrast, when $c_1 = 0$, from Eq. (42), Condition (a) does not exist for $u_2(t)$ to be bounded. Furthermore, even in the case $c_1 \neq 0$, since we assume that $k_1 > 0$ and $c_1 > 0$ throughout, Condition (a) is trivial. Since F_2 is the only applied force, one can artificially set it to satisfy Condition (b). The behavior of $f_1(t)$ needs further investigation. From Eq. (34), it can be determined that the following conditions must satisfy Condition (b).
(c) $y > 0$ and $\alpha > -1$, or $y < 0$ and $\alpha < -1$, so that there will be no exponentially growing behavior due to $f_1(0)$.
(d) $u_1(t)$ and $\dot{u}_1(t)$ must be non-exponentially growing functions.

In order to satisfy Condition (d), one needs to look into the solution of u_1, Eq. (45), carefully. It can be understood that the particular solution of u_1 will be bounded if F_2 is bounded and the driving frequencies are not equal to the resonant frequencies of the system (rigorously speaking, it is not the conventional resonant frequencies ($\approx \sqrt{K/M}$), but λ_1 and λ_2; see Eq. (47)). As for the homogeneous solution of u_1, one can derive the stability conditions from Eq. (47) as follows, with the definition of $y = \kappa k$. One of the following two conditions is enough to ensure the stability.
(e) $1 + \kappa + \frac{\kappa(1+\alpha)}{\gamma} > 0$ and $(1 + \kappa + \frac{\kappa(1+\alpha)}{\gamma})^2 - 4(\frac{\kappa(1+\alpha)}{\gamma} + \frac{\alpha\kappa^2}{\gamma}) < 0$.
(f) $1 + \kappa + \frac{\kappa(1+\alpha)}{\gamma} > 0$ and $(\frac{\kappa(1+\alpha)}{\gamma} + \frac{\alpha\kappa^2}{\gamma}) > 0$.

For the second equation in Condition (e), we have checked that α does not have purely real-number solutions in $\kappa = -100$ to 100, for $\gamma = 1, 10, 100, 1000$. Therefore, we conjecture that the inequality cannot be satisfied for a wide range of α, κ, and γ.

Consequently, Condition (e) will not be satisfied. Further analysis shows that Condition (f) can be replaced by the following two conditions.
(f1) $\kappa > 0$ and $\alpha > -\frac{\gamma}{\kappa} - \gamma - 1$, or $\kappa < 0$ and $\alpha < -\frac{\gamma}{\kappa} - \gamma - 1$, for the first inequality in (f).
(f2) $\kappa > 0$ and $\alpha\kappa + \alpha + 1 > 0$, or $-1 < \kappa < 0$ and $\alpha < -\frac{1}{1+\kappa}$, or $\kappa < -1$ and $\alpha > -\frac{1}{1+\kappa}$, for the second inequality in (f).

Conditions (f1) and (f2) have to be satisfied simultaneously to fulfill Condition (f). In contrast, when $c_1 = 0$, from Eq. (35), Condition (e) is not necessary, and Condition (f) must be replaced by the following one.
(g) $\frac{ky(1+\alpha)+\alpha y^2}{\eta(k+y)} > 0$.

Condition (g) can be further simplified as follows, with the definition of $y = \kappa k$, when $k/\eta > 0$.
(g') $1 + \kappa > 0$ and $\alpha\kappa^2 + \alpha\kappa + \kappa > 0$, or $1 + \kappa < 0$ and $\alpha\kappa^2 + \alpha\kappa + \kappa < 0$.

It can be shown that Condition (g') is equivalent to Condition (f2). In the case for $y < 0$ (negative stiffness in the standard linear solid element), Conditions $(c)_2$ and (e), or Conditions $(c)_2$, (f1), and (f2) must be satisfied to ensure bounded responses, as shown in Figure 3, the shaded area as an example of stability regimes with a negative stiffness element. The first quadrant of Figure 3 also indicates stability, corresponding to positive stiffness for all the elements.

5. Discussion. It is noted again that the parametric study here and in the following is based on the model shown in Figure 2(b). The stability map, as shown in Figure 3, is valid as long as the driving force, F_2, is a non-exponentially growing function and its driving frequency is not the natural frequency of the system. The dotted line indicates the asymptote of the stability boundary. From the stability analysis above, one can identify the stability regions as follows.
(I) $\kappa > 0$ and $\alpha > 0$ (not interesting, since positive stiffness for all the elements),
(II) $-1 < \kappa < 0$ and $\alpha < -\frac{1}{1+\kappa}$, and
(III) $\kappa < -1$ and $\alpha > -\frac{1}{1+\kappa}$, depending on γ.
The shaded area is the stable region for any γ. For the c-degenerate case, i.e., $c = 0$, γ must be set as large as possible to maintain finite η, the damping in the standard linear solid. In this case, case (III) does not depend on γ any more. However, it does not mean that the region, $\alpha > -\frac{1}{1+\kappa}$, is stable because of Condition (c). This result implies that if the response of the system at node 1 is stable, i.e., bounded, then that at node 2 is stable, as well. Thus, the trajectories of the symbols, solid square and open circle, coincide. One is the stability boundary and the other is the trajectory causing infinite compliance with $c = 0$ and $\eta = 0$ for the 1-dof case, i.e., $k_2 = 0$, $\eta_2 = 0$ (see Eq. (63) in Appendix B). As will be seen later, to achieve extreme high stiffness, one needs to be in the region where $\kappa < -1$.

Figure 4(a) shows the quasi-static response of the model in Figure 2(b) with respect to the negative stiffness element (y). The highest compliance at $y = -1.6$ kN/m is reached simultaneously for nodes 1 and 2 due to stiffness neutralization in Element 1. The lowest compliance (i.e., highest stiffness) occurs at about $y = -2.6$ kN/m. The real part of the compliance of the system at node 1 is negative when $y < -1.6$ kN/m, and that at node

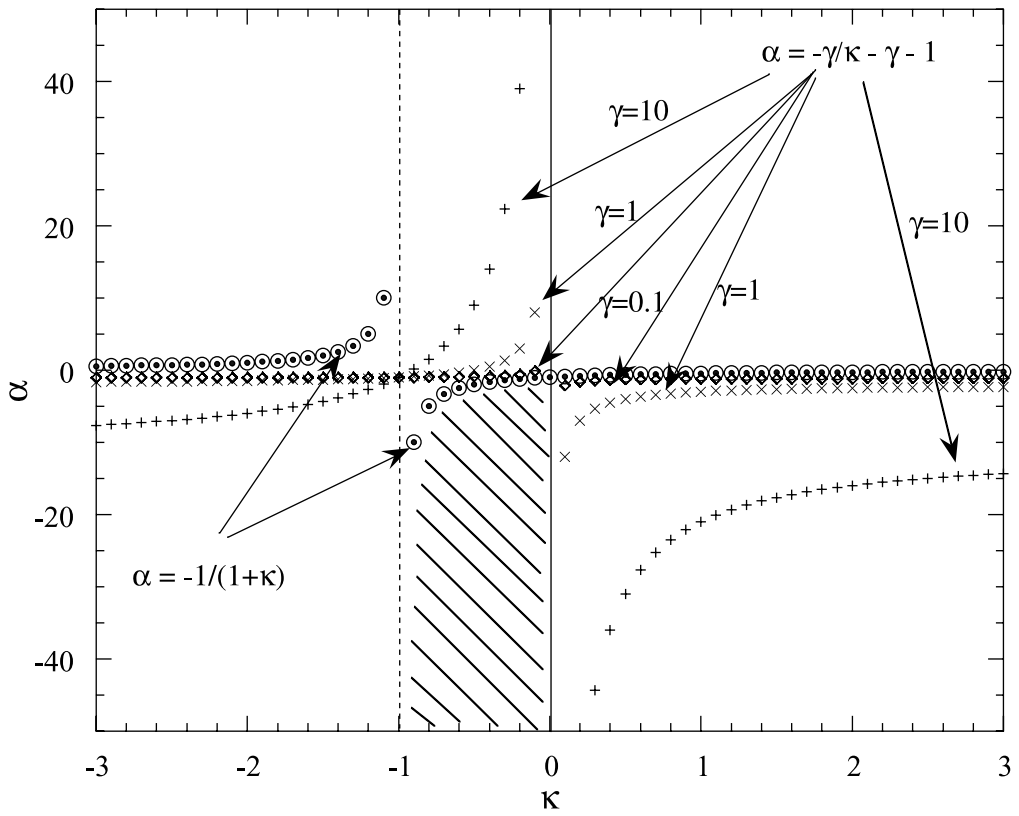

FIG. 3. Stability map for α, γ, and κ, based on the solutions of governing differential equations in time domain. The shaded region and the first quadrant (i.e., $\kappa > 0$ and $\alpha > 0$) correspond to stability.

2 is negative when $-2.6 < y < -1.6$ kN/m. The stability analysis based on Lyapunov's theorem shows a stable regime, as indicated in Figure 4(b). Since α is negative, the role of the negative stiffness element switches between the y- and z-springs, again by definition $z = \alpha y$. Thus, the system becomes unstable when $y > 0$ and $y < -1.6$ kN/m. The parameters η and ω are assumed to be 0.0001 kN-s/m and 0 rad/s, respectively, in both Figures 4 and 5. It is noted that for such a small viscosity η, a standard linear solid with no negative stiffness elements has a time constant ($\tau \approx$ viscosity/stiffness) on the order of 10^{-5} seconds, if the stiffness of spring elements is about 10 kN/m. Consequently, the Debye peak for the $\tan\delta$ of the standard linear solid will be at a frequency of about 10^5 rad/s. In Figure 5, we plot the compliance curves and the stability-losing eigenvalue with respect to the negative stiffness (y), for different $\alpha's$. It can be seen that the spacing between extreme high compliance and stiffness can be reduced by increasing α. But, the distance cannot be reduced arbitrarily much, as can be seen for large $\alpha's$. Also, the stability-losing eigenvalue has larger magnitude, indicating higher rate of divergence, i.e., more unstable, for large α. It is noted again that the stability boundary from previous analysis is at extreme high compliance.

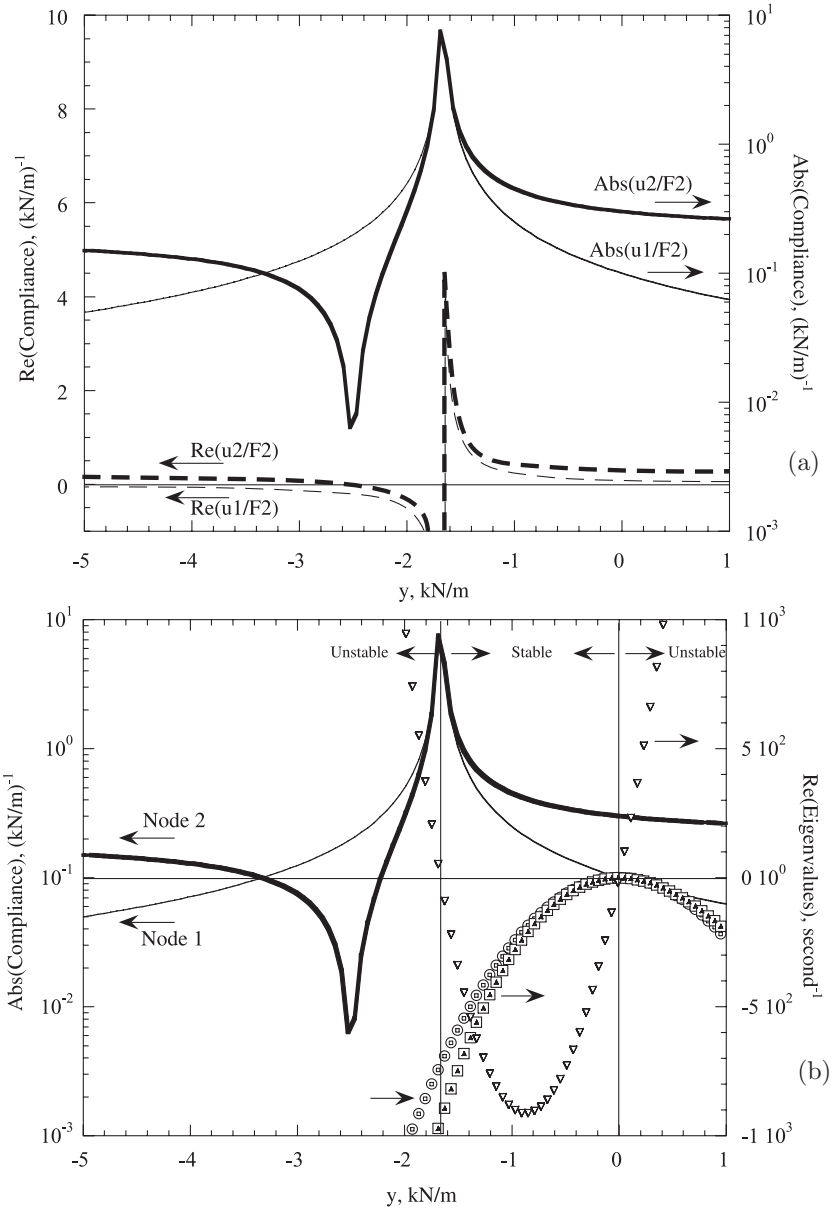

FIG. 4. Quasistatic behavior: no inertial terms. (a) Compliance, $\Re(\widetilde{u}_1/\widetilde{F}_2)$ and $\Re(\widetilde{u}_2/\widetilde{F}_2)$, on a linear scale (left) and absolute compliance, $|\widetilde{u}_1/\widetilde{F}_2|$ and $|\widetilde{u}_2/\widetilde{F}_2|$, on a logarithmic scale (right) vs. y with $\omega = 0$ and $\alpha = -1.2$. (b) Overall compliance and the stability-losing eigenvalue vs. y with $\omega = 0$ and $\alpha = -1.2$. We define $z = \alpha y$, where y and z are stiffness in Figure 2 (b) with $c_1 = 0$. The unstable branch for $y > 0$ is due to $\alpha < 0$.

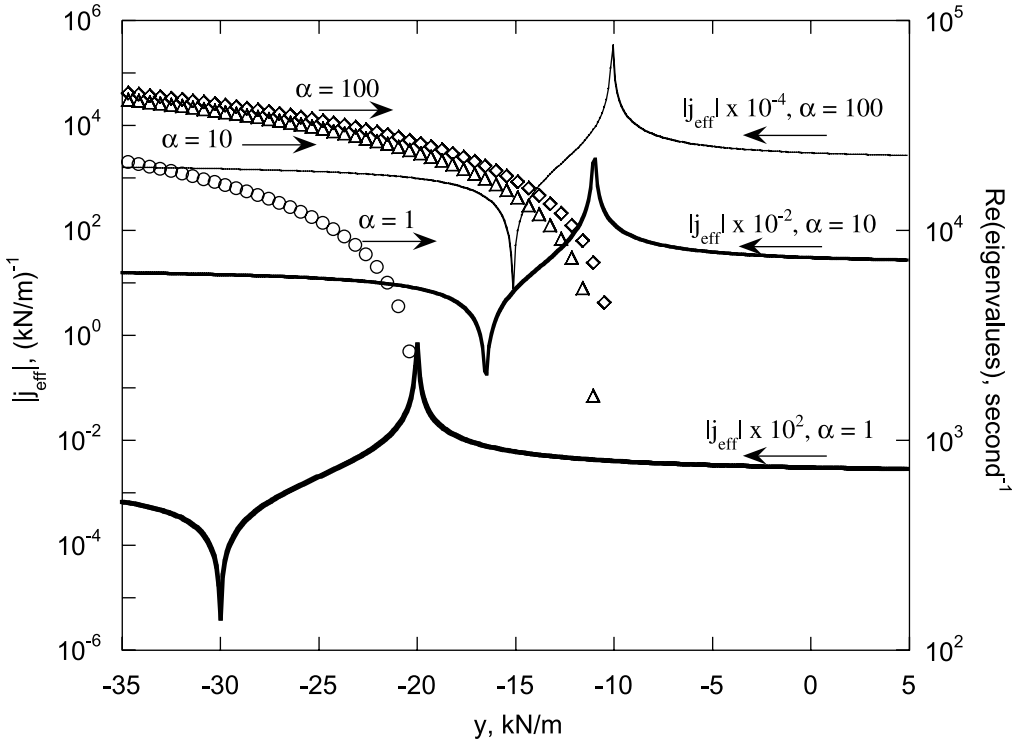

FIG. 5. Quasistatic behavior: no inertial terms. Effective compliance ($|j_{eff}|$) vs. negative stiffness (y) in the purely elastic limit with different $\alpha's$. $k_1 = 10, k_2 = 5$ kN/m, $m_1 = m_2 = 10^{-8}$ kg, $\eta = 0.0001$ kN-s/m and $\omega = 0$ rad/s. We define $z = \alpha y$, where y and z are stiffness in Figure 2 (b). For clarity, compliance curves are separated by multiplying by a constant.

In Figures 6, 7, and 8, we show the high frequency responses of the system under the influence of negative stiffness with $\eta = 0.0001$ kN-s/m and $\alpha = -5$. All peaks are structural resonant and anti-resonant frequencies. The purpose of studying high frequency responses is to understand the process of neutralization due to negative stiffness. Figure 6 shows the frequency response of compliance at discrete negative stiffness in y. It is noted when $y = -15$ kN/m, there is no anti-resonant-like behavior. In Figure 7, the peaks are also structural resonances for high frequency responses. It shows that the anti-resonant peaks (high stiffness) move to the low negative stiffness regime (i.e., in the stable zone, if negative stiffness is low enough), as driving frequency increases. Excessive negative stiffness makes anti-resonances disappear. From Figures 6 and 7, it also can be seen that by tuning either frequency or negative stiffness, one can alter the spacing between resonant and anti-resonant peaks, or even flip their order of appearance with respect to frequency or negative stiffness. We emphasize that at the low frequency limit the upward or downward peaks in compliance are not structural resonant phenomena, but at high frequency the peaks indicate the natural frequencies of the system. The shift in the natural frequency is due to cancellation in overall stiffness. The stability analysis of the

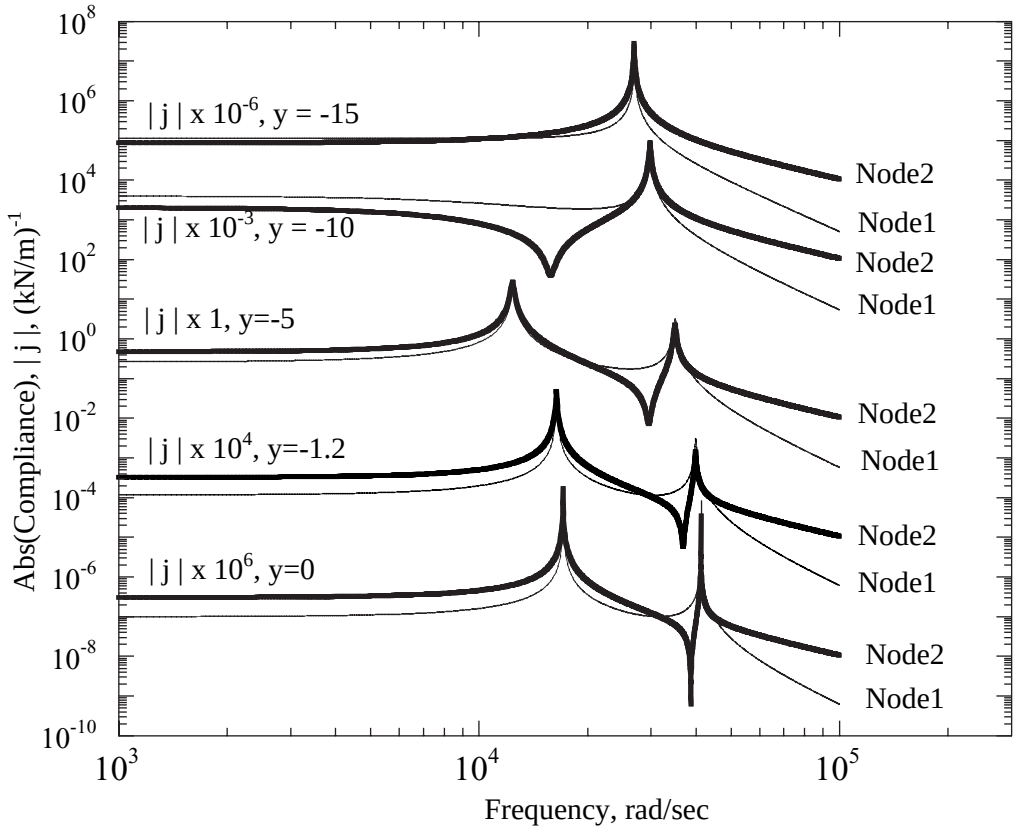

FIG. 6. Dynamic compliance vs. frequency with different negative stiffness (y) in units of kN/m. $m_1 = m_2 = 10^{-8}$ kg. $k_1 = 10, k_2 = 5$ kN/m, $\alpha = -5, \eta = 0.0001$ kN-s/m. Absolute compliances at node 1 and node 2 are calculated from $|\widetilde{u}_1/\widetilde{F}_2|$ and $|\widetilde{u}_2/\widetilde{F}_2|$, respectively. The symbol $|j|$ denotes compliance either at node 1 or node 2. Based on Figure 2(b) with $c_1 = 0$. The upward and downward peaks are structural resonances and anti-resonances, respectively. Thin solid lines are the compliance at node 1 and thick ones are the effective compliance of the system. For clarity, curves are separated by multiplying by a constant.

system driven at 25k rad/sec is shown in Figure 8, with respect to negative stiffness. It shows that the extreme high stiffness ($y = -7$ kN/m) is located in the stable regime. The result is not too surprising physically, because one can easily obtain extreme dynamical stiffness due to the structural anti-resonant response and negative stiffness plays a role to shift the structural anti-resonance, but the methodology is based on Lyapunov's indirect theorem. Again, the instability in the regime $y > 0$ is due to $\alpha < 0$. When $y < -7$ or $y > 0$, eigenvalues split. The eigenvalue whose real part is greater than zero causes the system to be unstable, as discussed in [12].

In Figure 9 (a), we plot the h and g function in Eqs. (27) and (28) to demonstrate the singularities in $\tan\delta$. This phenomena have been reported in [13] and [14]. Here, we

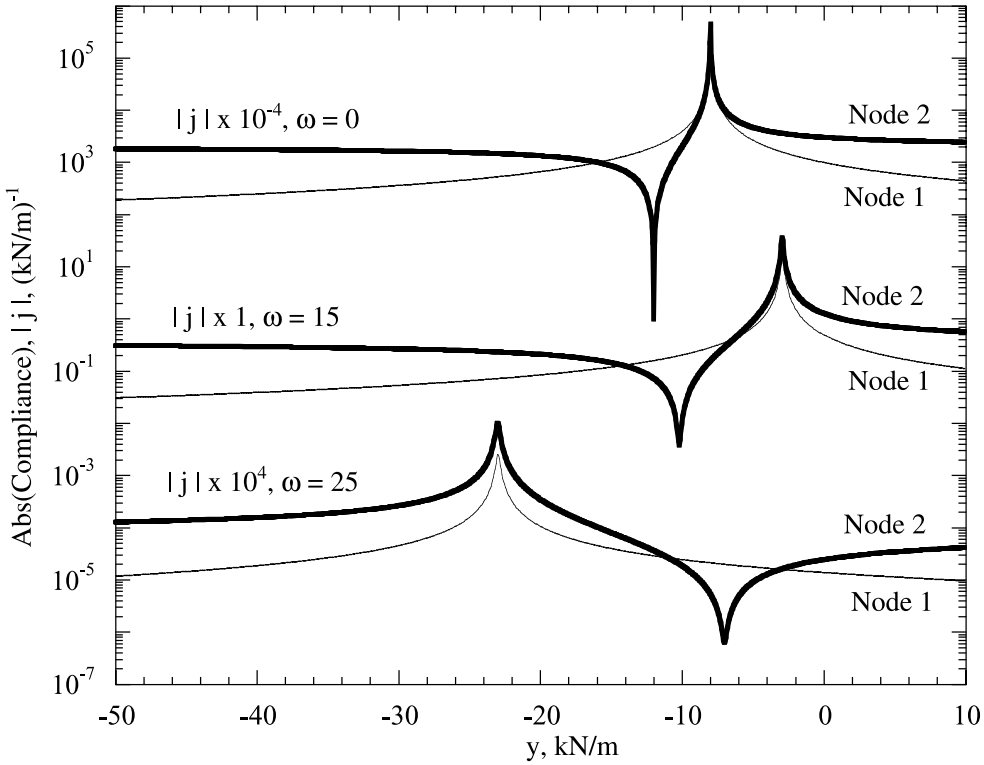

FIG. 7. Dynamic compliance vs. y with different frequencies. Frequency is in units of 10^3 rad/sec. $m_1 = m_2 = 10^{-8}$ kg. $k_1 = 10, k_2 = 5$ kN/m, $\alpha = -5$, $\eta = 0.0001$ kN-s/m. Absolute compliances at node 1 and node 2 are calculated from $|\widetilde{u}_1/\widetilde{F}_2|$ and $|\widetilde{u}_2/\widetilde{F}_2|$, respectively. The symbol $|j|$ denotes compliance either at node 1 or node 2. Based on Figure 2(b) with $c_1 = 0$. Peaks indicate structural resonances for high frequency responses. For clarity, curves are separated by multiplying by a constant.

mathematically investigate the behavior of $\tan\delta$ under the influence of negative stiffness. It is noted that in this analysis, we set $z = 5$ kN/m and $\omega = 1$ rad/sec. As seen, when η is small (less than about 0.4 kN-s/m), there are two zeros in the g function, indicating two singularities in $\tan\delta$, since the h function is finite, in the negative stiffness range plotted. When η is large, the singularities in $\tan\delta$ disappear and the $\tan\delta$ curve appears as a hump, as reported in [13] and [14]. In Figure 9 (b), we show that the stability boundary, calculated based on Lyapunov's indirect theorem, coincides at the right hand side of the first zero (from the origin) in g. It indicates that the singularities of $\tan\delta$ are located in the unstable (or metastable) regime. However, in a limiting case, as $\eta \to 0$, one can achieve stable singular $\tan\delta$.

6. Conclusions. We rigorously derive the stability criteria for the 2-dof viscoelastic system containing a negative stiffness element. The stability conditions derived from the time domain solutions of the differential systems are good for the response of the system

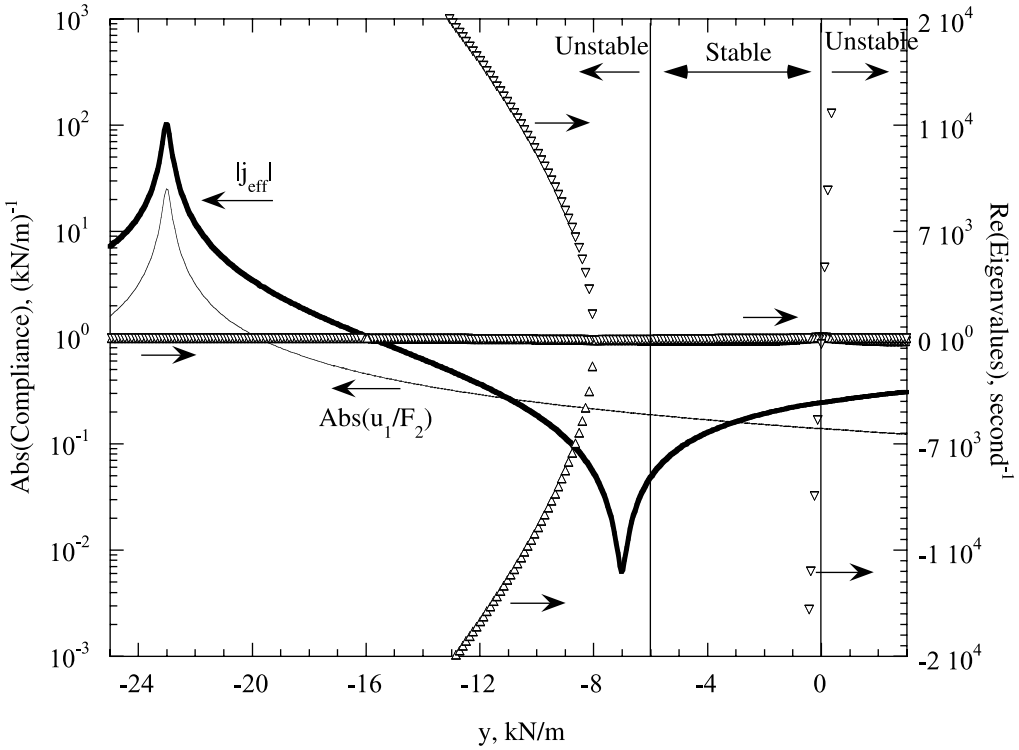

FIG. 8. Routh-Hurwitz eigenvalues and dynamic compliance vs. y, at $\omega = 25$k rad/sec. $m_1 = m_2 = 10^{-8}$ kg. $k_1 = 10, k_2 = 5$ kN/m, $\alpha = -5, \eta = 0.0001$ kN-s/m. Based on Figure 2(b) with $c_1 = 0$. The unstable branch for $y > 0$ is due to $\alpha < 0$.

at any frequency. Stable extreme stiffness at high frequency is demonstrated. Stable extreme $\tan\delta$ at low frequency is verified. In the low frequency limit, the system shows stable extreme high compliance and metastable extreme high stiffness.

7. Appendix A: A case of m-degeneracy. The purpose of this appendix is to demonstrate the effects of c-degeneracy and m-degeneracy. We consider the 1-dof viscoelastic model, as shown in Figure 10. The governing equation of the system can be expressed in the state-space representation, as follows.

$$\begin{pmatrix} \dot{u} \\ \dot{v} \\ \dot{f} \end{pmatrix} = \begin{bmatrix} 0 & 1 & 0 \\ -\frac{k}{m} & \frac{c}{m} & -\frac{1}{m} \\ \frac{\alpha y^2}{\eta} & y & -\frac{y(1+\alpha)}{\eta} \end{bmatrix} \begin{pmatrix} u \\ v \\ f \end{pmatrix} + \begin{pmatrix} 0 \\ \frac{F}{m} \\ 0 \end{pmatrix}. \tag{52}$$

It is understood that the characteristic equation of the Jacobian matrix in Eq. (52) is a complicated third-order polynomial. The solutions of the characteristic equation are the eigenvalues for the Lyapunov stability analysis. However, for $c = 0$ (c-degeneracy), one

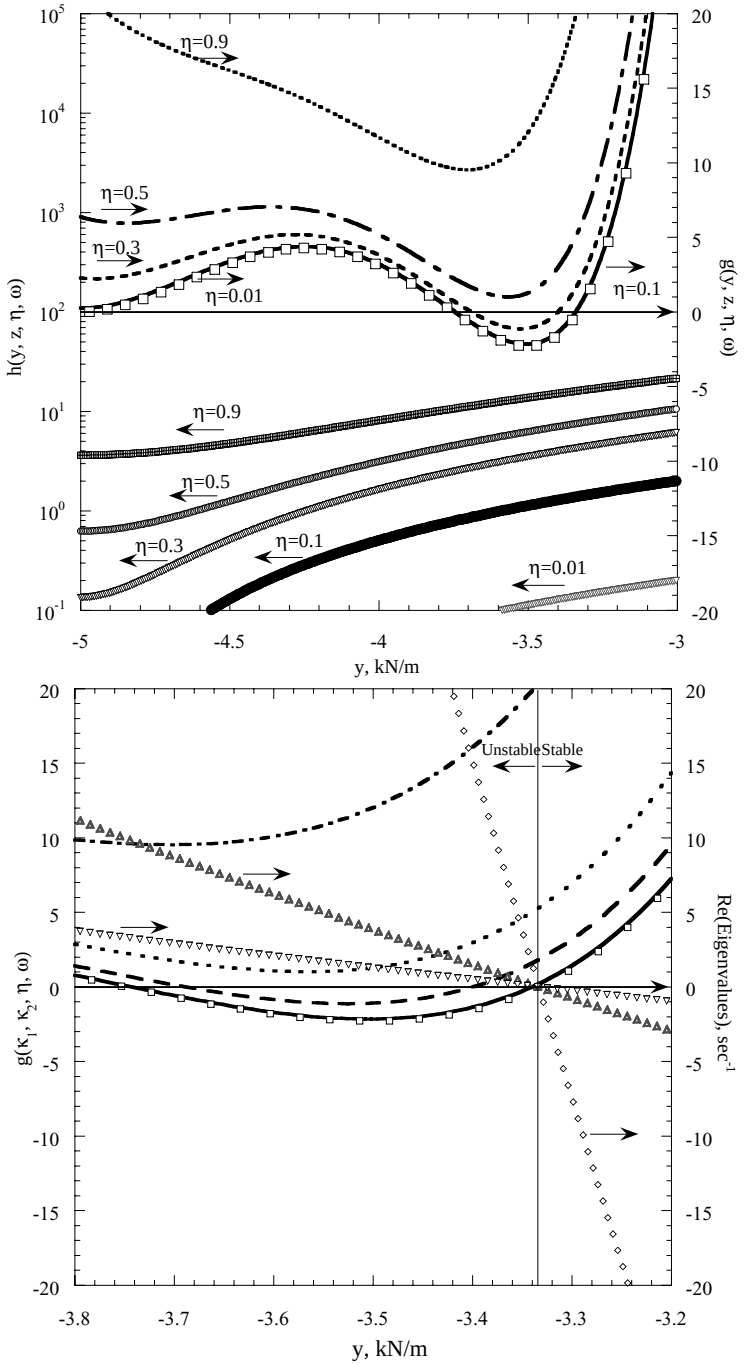

FIG. 9. Singularities in $\tan\delta$ and their stability, calculated with $k_1 = 10, k_2 = 5, z = 5$ kN/m, $\omega = 1$ rad/s. Based on Figure 2 (b) with $c_1 = 0$. (a) Singularities in $\tan\delta$. $g = 0$ indicates singularities. (b) Stability of the singularities in $\tan\delta$. Curved lines are calculated g function with respect to various η, defined in (a). Stability analysis is based on Eq. (51).

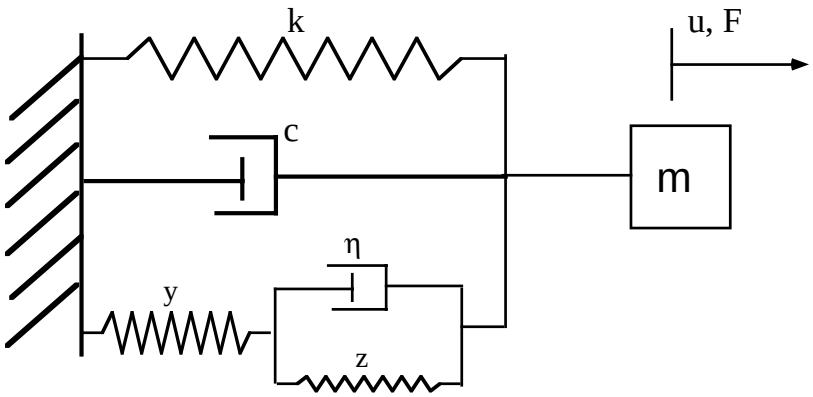

FIG. 10. One-dof viscoelastic model.

can write down the simpler characteristic equation as follows.

$$\lambda^3 + \frac{y(1+\alpha)}{\eta}\lambda^2 + (\frac{k}{m} + \frac{y}{m})\lambda + \frac{\alpha y^2}{m\eta} + \frac{y(1+\alpha)}{m\eta} = 0. \tag{53}$$

However, if one further assumes $m = 0$ (m-degeneracy), the characteristic equation becomes

$$\lambda = \frac{k(\alpha\kappa^2 + \alpha\kappa + \kappa)}{\eta(1+\kappa)}. \tag{54}$$

As seen, from Eq. (53) to (54), the numbers of roots of the characteristic decrease from 3 to 1, which means that there is some information missing for stability analysis due to degeneracies.

8. Appendix B: Further demonstration through a 1-DOF viscoelastic model. The purpose of this appendix is to show the statement made in the first paragraph in the discussion. Consider the mechanical model shown in Figure 10. The corresponding governing equations in time domain are as follows, when $m = 0$.

$$ku + c\dot{u} + f = F, \tag{55}$$

$$f + \frac{\eta}{y+z}\dot{f} = \frac{yz}{y+z}u + \frac{y\eta}{y+z}\dot{u}, \tag{56}$$

where $y = \kappa k, z = \alpha\kappa k$, and $\eta = \gamma c$. The symbol f denotes the internal force in the standard linear element. Through Fourier transform, the governing equations in the

frequency domain are

$$(k + ic\omega)\widetilde{u} + \widetilde{f} = \widetilde{F}, \tag{57}$$

$$(y + z + i\omega\eta)\widetilde{f} = (yz + i\omega y\eta)\widetilde{u}. \tag{58}$$

One can calculate the effective compliance as follows.

$$\frac{\widetilde{u}}{\widetilde{F}} = \frac{A}{A^2 + B^2} - i\frac{B}{A^2 + B^2}, \tag{59}$$

where

$$A = k + k_1\frac{\alpha(1+\alpha) + \omega^2\beta^2}{(1+\alpha)^2 + \omega^2\beta^2}, \tag{60}$$

$$B = \omega c(1 + \frac{\gamma}{(1+\alpha)^2 + \omega^2\beta^2}), \quad and \tag{61}$$

$$\alpha = k_2/k_1, \beta = \eta/y, \gamma = \eta/c. \tag{62}$$

For $c = \eta = 0$, i.e., $B = 0$, the extreme (infinite) compliance occurs at $A = 0$, i.e.,

$$y = -\frac{1+\alpha}{\alpha}. \tag{63}$$

For a fixed k, one can draw two hyperbolic curves on the $\alpha - y$ plane. To derive the solution of Eq. (55) and (56) in time domain directly, we first rewrite the governing equation in the following way.

$$c\ddot{u} + (k + y + \frac{y(1+\alpha)}{\gamma})\dot{u} + (\frac{ky(1+\alpha)}{\gamma c} + \frac{\alpha y^2}{\gamma c})u = \frac{y(1+\alpha)}{\gamma c}F + \dot{F}. \tag{64}$$

The general solution of Eq. (64) is as follows.

$$u = u^h + u^p. \tag{65}$$

The homogeneous solution is

$$u^h = C_1 e^{\lambda_1 t} + C_2 e^{\lambda_2 t}, \tag{66}$$

where C_1 and C_2 are determined by initial conditions and

$$\lambda_{1,2} = \frac{-(k + y + \frac{y(1+\alpha)}{\gamma}) \pm \sqrt{(k + y + \frac{y(1+\alpha)}{\gamma})^2 - 4(\frac{ky(1+\alpha)}{\gamma} + \frac{\alpha y^2}{\gamma})}}{2c}. \tag{67}$$

The positive real part of $\lambda's$ indicates that the homogeneous solution, u^h, becomes unbounded as time increases, which is unstable in the sense of Routh-Hurwitz. In order to obtain stable (non-growing) solutions, one of the following two sets of inequalities must be satisfied, for $k > 0$. Let $y = \kappa k$ and $c \neq 0$.
(B-1) $1 + \kappa + \frac{\kappa(1+\alpha)}{\gamma} > 0$ and $(1 + \kappa + \frac{\kappa(1+\alpha)}{\gamma})^2 - 4(\frac{\kappa(1+\alpha)}{\gamma} + \frac{\alpha\kappa^2}{\gamma}) < 0$. It is conjectured that the second inequality will not hold for a wide range of α, γ, and κ.
(B-2) $1 + \kappa + \frac{\kappa(1+\alpha)}{\gamma} > 0$ and $(\frac{\kappa(1+\alpha)}{\gamma} + \frac{\alpha\kappa^2}{\gamma}) > 0$.

As seen, Condition (B-2) here is the same as Condition (f) in the 2-dof case. Figure 11 shows the compliance curves, based on Eq. (59), and the results from Lyapunov's stability analysis. It shows that if the amount of negative stiffness is more than that corresponding to the highest compliance, the system will be unstable. Since negative α is used in the graph, there is another unstable branch when y is sufficiently positive.

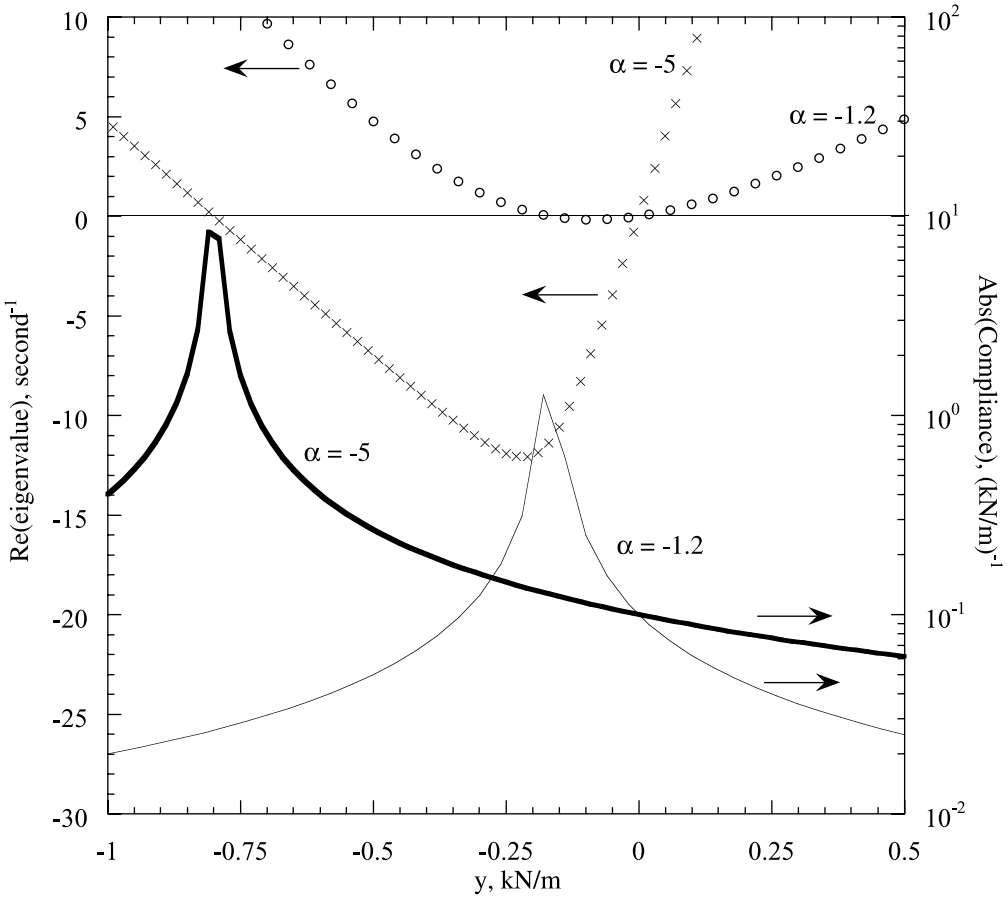

FIG. 11. Compliance and eigenvalue analysis of the 1-dof system in Figure 10.

REFERENCES

[1] R. Bulatovic, On the Lyapunov stability of linear conservative gyroscopic systems, C. R. Acad. Sci. Paris, t. 324, Serie II b, p. 679-683 (1997).

[2] P. Gallina, About the stability of non-conservative undamped systems, Journal of Sound and Vibration, 262, 977-988 (2003). MR1971816 (2004b:70044)

[3] R. S. Lakes, "Extreme damping in composite materials with a negative stiffness phase", Physical Review Letters, 86, 2897-2900 (26 March 2001).

[4] R. S. Lakes, "Extreme damping in compliant composites with a negative stiffness phase" Philosophical Magazine Letters, 81, 95-100 (2001).

[5] R. S. Lakes, T. Lee, A. Bersie, and Y. C. Wang, "Extreme damping in composite materials with negative stiffness inclusions", Nature, 410, 565-567 (29 March 2001).

[6] R. S. Lakes and W. J. Drugan, Dramatically stiffer elastic composite materials due to a negative stiffness phase?, J. Mechanics and Physics of Solids, 50, 979-1009 (2002).

[7] H. Leipholz, Stability of elastic systems, Sijthoff & Noordhoff, Alphen aan den Rijn, The Netherlands, 1980. MR0595163 (82g:73001b)

[8] L. Meirovitch, Methods of Analytical Dynamics, McGraw-Hill, New York, 1970.

[9] J. W. Morris Jr. and C. R. Krenn, The internal stability of an elastic solid, Philosophical Magazine A, 80, 12, 2827-2840 (2000).

[10] S. H. Strogatz, Nonlinear Dynamics and Chaos, Perseus Books, Cambridge, Massachusetts, 1994.
[11] Y. C. Wang and R. S. Lakes, Extreme thermal expansion, piezoelectricity, and other coupled field properties in composites with a negative stiffness phase, J. Appl. Phys. 90, 6458-6465 (2001).
[12] Y. C. Wang and R. S. Lakes, Extreme stiffness systems due to negative stiffness elements, American Journal of Physics, 72, 40–50 (2004a).
[13] Y. C. Wang and R. S. Lakes, Stable extremely high-loss discrete viscoelastic systems due to negative stiffness elements, Appl. Phys. Lett. 84, 4451–4453 (2004b).
[14] Y. C. Wang and R. S. Lakes, Negative Stiffness Induced Extreme Viscoelastic Mechanical Properties: Stability and Dynamics, Philos. Mag., accepted (2004c).